CERVICAL CORD LESION CHARACTERISATION IN MULTIPLE SCLEROSIS (MS): A PILOT STUDY WITH APPLICATION TO MTR

Marios C Yiannakas[1], Hugh Kearney[1], Olga Ciccarelli[2], David H Miller[1], and Claudia A.M Wheeler-Kingshott[1]
[1]*Neuroinflammation, UCL Institute of Neurology, London, United Kingdom,* [2]*Brain Repair and Rehabilitation, UCL Institute of Neurology, London, United Kingdom*

INTRODUCTION: Multiple sclerosis (MS) lesions can be pathologically heterogeneous, with different degrees of inflammation, demyelination, remyelination, axonal loss and gliosis. Conventional MRI sequences are not able to reflect these complex pathological changes, but MS lesions detected on both PD/T2- and T1-weighted scans in the brain often reflect more severe tissue damage than lesions seen on PD/T2-weighted scans only [1, 2]. Magnetisation transfer ratio (MTR) is thought to reflect the integrity of myelin and axons, and differences in MTR have been found between brain lesions seen on T1- and PD/T2-weighted scans [1]. However, there is limited information regarding MTR values in spinal cord lesions. Given the importance of T1-weighted brain lesions (suggesting axonal loss) [4] and spinal cord pathology to physical disability [5], we evaluated cervical cord lesions using images acquired with different contrast mechanisms (T1- and PD-weighted scans). In addition, we assessed whether there were differences in the MTR between lesions seen with different sequences and between patients' normal appearing white matter (NAWM) and white matter of controls. Our hypothesis was that cord lesions seen on both PD- and T1-weighted scans would show lower MTR values than those visible only on PD-weighted scans, reflecting a more severe tissue damage and axonal loss.

METHOD: A) Study participants: 4 MS patients (mean age 44, 3 female, 1 male) and 4 healthy controls were recruited (mean age 34 years, 3 male, 1 female). Written informed consent was obtained from all participants and the study was approved by the local institutional review board. B) MR Imaging: using a 3T Philips Achieva MRI system with RF multi-transmit technology (Philips Healthcare, Best, Netherlands) and a 16-channel neurovascular (NV) coil, the cervical cord was imaged in the axial plane (i.e. slices perpendicular to the cord) with the center of the imaging volume at the level of C2-3 intervertebral disc. Scanning parameters: (i) PD-weighted (PDw) 3D-FFE: TR = 23 ms; TE = 5ms; flip angle α= 7°; FOV = 240 x 180 mm^2; voxel size = 0.5 x 0.5 x 5 mm^3; NEX = 8; 10 axial contiguous slices; scanning time = 13:34 min; (ii) T1-weighted (T1w) 3D-TFE: TR = 12 ms; TE = 6.1 ms; flip angle α = 8°; FOV = 512 x 256 mm^2; voxel size = 0.5 x 0.5 x 5 mm^3; NEX = 3; 10 slices; with PSIR (flip angle α = 5°); scanning time = 7:46 min; (iii) 3D-FFE with and without MT-weighting for MTR calculation: TR=36ms, two echoes with TE1 / TE2 = 3.5 / 5.9 ms, flip angle α =9°; FOV = 240 x 180 mm^2; acquisition matrix 240 x 320 (voxel size 0.75 x 0.75 mm^2, reconstructed to 0.5 x 0.5 mm^2); SENSE acceleration factor = 2; 22 axial contiguous slices matching the geometry of (i) and (ii); scanning time 15 min. MT pulse: Sinc - Gaussian shape; nominal α = 360º; offset frequency 1 kHz; duration 16 ms. The total acquisition time for the entire imaging protocol was approximately 45 min. In order to minimise the effect of motion during imaging, the neck was immobilised using an adjustable MR-compatible cervical collar, similar to the ones most commonly used in cases of whiplash injury. C) Image analysis: for each one of the 4 MS patients a 30 mm section of the cervical spine (i.e. 6 slices), centered at the C2-3 intervertebral disc, was analysed by extracting 6 matching slices using Jim (Xinapse systems, www.xinapse.com) from the PDw 3D-FFE, T1w 3D-TFE, the MT-off and MT-on volumes. All images were registered using a linear registration algorithm (flirt) from the fsl library (http://www.fmrib.ox.ac.uk/fsl/) as follows: the MT-off and MT-on images were independently registered to the PDw 3D-FFE prior to the calculation of the MTR-map. This was done in order to account for a possible change in the cord position during the acquisition of MT-off and MT-on. The T1w 3D-TFE was also registered to the PDw 3D-FFE so that all images including the MTR-map were in the same image space as the PDw 3D-FFE. Lesions were manually contoured using Jim and the PDw 3D-FFE and T1w 3D-TFE regions of interest (ROIs) were used to calculate the lesion volumes for each contrast. In addition, separate volumes were calculated for lesions only visible on PDw 3D-FFE and for lesions only visible on T1w 3D-TFE. Normal appearing white matter (NAWM) and normal appearing grey matter (NAGM) ROIs of a predefined size of 3 mm^2 were also segmented for each patient. Binary masks of all ROIs were created and applied to the MTR-map to obtain tissue-specific MTR measurements. In order to sample healthy tissue MTR values, a similar processing pipeline was used for the healthy controls. For the healthy control data, a 15 mm section through the C2-3 intervertebral disc was extracted from the PDw 3D-FFE, the MT-on and MT-off datasets. The MT-on and MT-off were independently registered with the PDw 3D-FFE (prior to the calculation of MTR-map). The mean MTR values of total grey matter (TGM) and total white matter (TWM) volumes was measured as follows: the total cord volume (TCV) was segmented from the 3D-FFE using the active surface model as previously reported [6] and TGM volume was segmented from the same image with a semi-automated method that uses the fuzzy connector tool [7]. TWM volume was calculated from the difference between TCV and TGM. Masks of TWM and TGM were then applied to the MTR-maps for mean MTR estimation. D) Statistical analysis: the Wilcoxon and Mann Whitney tests were used (SPSS 11.0, Chicago, Ill., USA) to check for differences in MTR values between groups.

RESULTS: PDw 3D-FFE images allowed visualisation of larger volumes of abnormal tissue than T1w 3D-TFE (Figure 1, Table 1). Table 2 shows the MTR values of lesions (for each type of image contrast) for each MS patient individually as well as the mean MTR measures for all patients combined. The mean WM and GM MTR values in the 4 healthy controls combined were 52.9 ± 0.6 and 50.8 ± 0.6, respectively. No significant difference in MTR was found between lesions seen on the T1w and PDw images. In addition, no significant difference in MTR was found between patients' NAWM and WM in healthy controls. However, the MTR of NAGM in patients was significantly lower than that of healthy GM (*p*-value = 0.02).

Table 1	T1w 3D-TFE mean lesion volume (mm^3)	PDw 3D-FFE mean lesion volume (mm^3)
Case 1	686	695.5
Case 2	158	243.5
Case 3	616	633.5
Case 4	126	339.5

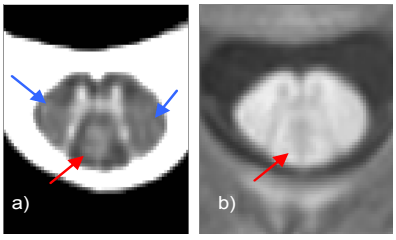

Figure 1. a) An example of a 3D-FFE and b) 3D-TFE images. Arrows indicate lesional areas visible on both images (red) or just the 3D-FFE (blue).

Table 2	T1w 3D-TFE mean lesion MTR (T1w lesions only)	PDw 3D-FFE mean lesion MTR (PDw lesions only)	NAWM – Mean MTR	NAGM – Mean MTR
Case 1	47 (47)	47 (49)	51.5	47.5
Case 2	46.5 (47)	48 (49)	50.5	46.5
Case 3	41 (41)	41 (44)	51.5	44.5
Case 4	48 (48)	49 (50)	53	48
Mean (± SD)	44.5 (4.2)	46.4 (4.5)	51.6 (1.0)	46.6 (1.5)

CONCLUSION: This pilot study defines a protocol from acquisition to analysis, allowing for the first time characterisation of MTR values of spinal cord lesions in MS using images acquired with different contrast mechanisms. Although a small heterogeneous cohort was studied, no significant differences were found in MTR values of PDw and T1w lesions, therefore our preliminary results suggest that spinal cord lesions appear more homogenous than those in the brain. However, PDw does enable the visualisation of a larger volume of abnormal tissue compared to T1w scans of the cord. Significantly lower MTR values were seen in the NAGM compared to controls, despite the apparent absence of lesions on these images (pathological studies have previously shown the presence of a significant number of lesions in GM). Further studies will increase the sample size and aim to improve visualization of GM lesions in the spinal cord.

REFERENCES: 1) vanWaesberghe et al, (1999), Ann Neurol, 46 (5): 747-54. 2) vanWalderveenMA et al, (1998), Neurology, 50: 1282–1288. 3) Lycklama a Nijeholt GJ et al, (2000), J Neuroimaging, 10 (2): 67-72. 4) Agosta et al, (2007), Arch Neurol, 64 (9): 1302-1305. 5) Koopmans et al, (1996), Neurology, 47: 1469-76. 6) Horsfield M, A et al, (2010), Neuroimage, 50: 446-455. 7) Udupa JK, Samarasekera S. (1996), Graphical Models and Image Processing, 58: 246-261.
ACKNOWLEDGEMENTS: MS Society of Great Britain and Northern Ireland and CBRC for funding.